Gene expression profiling-based identification of cell-surface targets for developing multimeric ligands in pancreatic cancer

Yoganand Balagurunathan,[1] David L. Morse,[2]
Galen Hostetter,[1] Vijayalakshmi Shanmugam,[1]
Phillip Stafford,[1] Sonsoles Shack,[1] John Pearson,[1]
Maria Trissal,[3] Michael J. Demeure,[1,4]
Daniel D. Von Hoff,[1] Victor J. Hruby,[5]
Robert J. Gillies,[3] and Haiyong Han[1]

[1]Translational Genomics Research Institute, Phoenix, Arizona
and [2]BIO5 Institute, [3]Arizona Cancer Center and Department of
Radiology, [4]Department of Surgery, College of Medicine,
and [5]Department of Chemistry, The University of Arizona,
Tucson, Arizona

Abstract

Multimeric ligands are ligands that contain multiple binding domains that simultaneously target multiple cell-surface proteins. Due to cooperative binding, multimeric ligands can have high avidity for cells (tumor) expressing all targeting proteins and only show minimal binding to cells (normal tissues) expressing none or only some of the targets. Identifying combinations of targets that concurrently express in tumor cells but not in normal cells is a challenging task. Here, we describe a novel approach for identifying such combinations using genome-wide gene expression profiling followed by immunohistochemistry. We first generated a database of mRNA gene expression profiles for 28 pancreatic cancer specimens and 103 normal tissue samples representing 28 unique tissue/cell types using DNA microarrays. The expression data for genes that encode proteins with cell-surface epitopes were then extracted from the database and analyzed using a novel multivariate rule-based computational approach to identify gene combinations that are expressed at an efficient binding level in tumors but not in normal tissues. These combinations were further ranked according to the proportion of tumor samples that expressed the sets at efficient levels. Protein expression of the genes contained in the top ranked combinations was confirmed using immunohistochemistry on a pancreatic tumor tissue and normal tissue microarrays. Coexpression of targets was further validated by their combined expression in pancreatic cancer cell lines using immunocytochemistry. These validated gene combinations thus encompass a list of cell-surface targets that can be used to develop multimeric ligands for the imaging and treatment of pancreatic cancer. [Mol Cancer Ther 2008;7(9):3071–80]

Introduction

Using peptide-based ligands to target imaging or therapeutic agents to the surface of tumor cells is an actively investigated area of research. Several such ligands were developed and have shown very promising results in animal models and, in some cases, were successfully tested in humans. A series of RGD peptide-based ligands coupled with a variety of proteins, peptides, small molecules, nucleic acids, and radiotracers were developed to deliver therapeutics and imaging agents to tumor vasculature (1). Recently, the [^{18}F]galacto-RGD ligand was tested in humans and showed highly desirable pharmacokinetics and good visualization of the $\alpha_v\beta_3$-integrin expression with positron emission tomography scanning (2, 3). Radio-labeled monoclonal antibodies that target cell-surface antigens have been approved for the treatment of B-cell non-Hodgkin's lymphoma (4). However, results of using such antibody conjugates in the treatment of solid tumors are less encouraging (5, 6).

One major limitation of monomeric ligand-based agents is that the cell-surface targets must be highly expressed in tumor cells relative to normal tissues, which rarely occurs. As a possible solution, several groups are developing multivalent ligands containing multiple binding domains that target two or more separate proteins on the cell surface (7–12). Most multimeric ligands developed have been homomultimers (7, 10). Heteromultivalent ligands have also been attempted (9). Recently, we prepared hetero-dimeric ligands that simultaneously targeted both human δ-opioid and melanocortin receptors, which showed up to a 50-fold increase in binding (13).

One challenge facing the development of multivalent ligands is the identification of cell-surface target combinations that are expressed concurrently in tumor cells but not in normal cells. It is conceivable that a single target will only be expressed in a fraction of patients' tumors. It is therefore very likely that there will be even less of a percentage of patients' tumors expressing a combination of targets. This suggests that a collection of multimeric ligands might be needed to treat all patients with the same general classification of disease, e.g. pancreatic cancer. Therefore, the successful development of a therapeutically useful

multimeric ligand requires a systematic approach to identify combinations of cell-surface targets that may be broadly applicable over large subsets of patients.

The ideal approach to identify protein targets would be a systematic direct survey comparing cell-surface protein levels in normal and tumor tissues. Although advances in proteomic technology have made it possible for genome-wide protein profiling, it is still very difficult to completely and quantitatively elucidate all cell-surface proteins. The main technological pitfall is that the majority of cell-surface proteins are either plasma membrane bound or integral to the membrane, which renders the traditional two-dimensional gel electrophoresis ineffective in resolving them. Recent reports describe new affinity tagging or radioisotope labeling to separate cell-surface proteins from other cellular proteins. The number of cell-surface proteins detected by these methods varies dramatically from a few to several hundred depending on sample and detection methods used (14, 15). The number of plasma membrane proteins that can be measured quantitatively is even smaller (16). Overall, only a small percentage of cell-surface proteins can be quantitatively detected by the most advanced proteomics technology currently available. Additional difficulties occur when applying proteomic analysis directly to tissue samples (17).

DNA microarray, a systematic approach for detecting mRNA transcripts, is considerably more mature compared with the current proteomics technology and is thus an attractive alternative for identifying expression of cell-surface proteins. Nonetheless, there are potential limitations in using DNA microarrays to identify cell-surface targets. For instance, it is generally known that mRNA and protein levels are not necessarily correlated. However, there is some evidence to indicate that levels of transcript and protein may have a greater correlation for cell-surface gene products compared with products localized in other parts of the cell. Loyet et al. found that, in human primary T helper cells, only 6 of 38 (16%) of membrane proteins showed differences between protein and transcript levels (16). Although it is impossible to eliminate these limitations, we postulated that by performing secondary validation assays at the protein level, such as immunohistochemistry, they could be greatly alleviated.

Herein, we describe the development of a multivariate computational method for identifying target combinations. Using this method, we have identified a list of lead target combinations that can be used for the development of multimeric ligands. Targets of two different combinations were validated using tissue microarray (TMA)-based immunohistochemistry and were further validated by quantifying their combined expression in pancreatic cancer cell lines.

Materials and Methods

Tissue Specimens and RNA Samples

Eight fresh-frozen pancreatic adenocarcinoma (PanAdo) tissues and four normal pancreas tissues were obtained from the Tissue Acquisition Shared Service at the Arizona Cancer Center. Microarray data for a second set of 20 PanAdo tissue samples were obtained from the Molecular Profiling Institute. RNA samples for normal tissues representing 28 different organ sites were purchased from Biochain and Stratagene. Paraffin-embedded pancreatic tissues were obtained from the Biospecimen Repository Core of the Pancreatic Cancer P01 project (CA109552) at Translational Genomics Research Institute. All tissues samples were provided without patient identifiers or personal information, and an institutional review board exemption was obtained for their use.

Gene Expression Analysis Using DNA Microarrays

Total RNA was isolated from fresh-frozen tissues using the RNeasy kit (Qiagen). Microarray analyses, including target labeling and chip hybridization and processing, were carried out following the manufacturer's recommended protocols (Agilent Technologies). Briefly, 1 μg total RNA was used to generate CY5 cRNA targets using the Agilent low-input RNA fluorescent linear amplification kit. RNA samples isolated from normal pancreas were labeled with CY3 to serve as a reference. In some cases, normal tissues were run on the CY3 channel and a tumor sample (from the same organ type as the normal tissue) was run on the CY5 channel. The concentration and integrity of fluorescent cRNA were analyzed using the Agilent 2100 Bioanalyzer. Equal amounts of labeled cRNA targets from the sample and the reference were then hybridized onto the Agilent Human 1A oligonucleotide arrays. Hybridization signals were acquired and normalized using Agilent's Feature Extraction software (version 7.1). DNA microarray profiles for pancreatic cell lines, obtained from the American Type Culture Collection, were generated by the same procedure using total RNA isolated from cells grown to ~80% confluence.

Compilation of a Cell-Surface Gene Database

A list of genes encoding proteins with cell-surface epitopes was compiled by first manually browsing through the entire Gene Ontology hierarchical vocabulary using the Cancer Genome Anatomy Project Gene Ontology browser. Each category was followed through the hierarchy to the lowest possible level to select lists of genes encoding proteins with cell-surface epitopes while excluding lists that did not include cell-surface proteins. A combined list of 6,389 genes was compiled. Genes that are not represented on the Agilent Human 1A arrays were removed and the resulting list contained 4,407 genes. Each of those genes was manually checked using information from existing databases (Genecard, Harvester, Entrez, Protein Database, and UniProt) to assure they encode cell-surface proteins. Genes known to encode or predicted to encode cell-surface products by similarity/homology were retained. Those known not to be cell surface, or if the subcellular localization was not determinable, were removed. Our final list contains a total of 2,177 genes on the Agilent Human 1A V2 and 1,928 genes on the 1A V1 chip (Supplementary Table S1).[6]

---

[6] Supplementary material for this article is available at Molecular Cancer Therapeutics Online (http://mct.aacrjournals.org/).

Cluster Analysis

Hierarchical clustering (agglomerative procedure) was used to generate dendrograms from the median normalized microarray expression data by assembling all tissue samples into a single tree based on their similarities. The clustering algorithm was based on the average-linkage method as described previously (18). Because our tissue samples included 28 normal tissue types and the PanAdo tissue group, the repetitive clustering process was stopped when 29 groups were formed.

TMA Construction and Immunohistochemistry

Formalin-fixed paraffin-embedded tissues were first examined with H&E staining using whole sections to identify pathologically distinct areas of interest (tumor, adjacent normal, and normal). TMAs were constructed by punching 1.0 mm discs and reembedding them into a new paraffin block (19–22). Each TMA block was cut into 5 μm sections and H & E staining was done on every 50th section to assess retention of desired pathologies. TMA slides for normal tissues in 0.6 mm spot sizes (version CHTN2002N1) were provided by the Cooperative Human Tissue Network funded by the National Cancer Institute/NIH.

To optimize staining conditions, antibodies were titrated against regular tissue sections and "tester" TMA slides containing a variety of tumor and normal tissues. TMA slides were first subjected to antigen retrieval by heating at 100°C in citrate buffer (0.1 mol/L, pH 6.0) for 5 to 30 min depending on the antibody. Slides were then incubated with primary antibodies at optimal dilutions for 30 min at room temperature. Biotinylated secondary antibodies were applied followed by streptavidin-peroxidase complex (Vision BioSystems) and resolved with diaminobenzidine chromogen. Stained slides were evaluated using light microscopy and scored (0 = negative to 3+ = intensely positive) by a board-certified pathologist (G.H.). Primary antibodies and dilutions used were rabbit anti-protein tyrosine phosphatase receptor type R (PTPRR; Orbigen), 1:100; rabbit anti-solute carrier family 2, member 13 (SLC2A13; US Biological), 1:300; mouse anti-protocadherin β10 (PCDHB10; Abnova), 1:75; and rabbit anti-interleukin-1 receptor accessory protein (IL1RAP; Abcam), 1:150.

Quantitative Real-time Reverse Transcription-PCR

Quantitative real-time reverse transcription-PCR was done as described previously (23) with the following changes. Primer sets were designed to generate cDNA and perform reverse transcription-PCR from ACTB (β-actin), IL1RAP, PCDHB10, PTPRR, and SLC2A13 mRNA. PCR conditions were determined so that maximum yield without spurious priming was achieved. Reverse transcription-PCR was conducted using a Smart Cycler (Cephid) and the QuantiTect SYBR Green reverse transcription-PCR kit (Qiagen). As controls, a no reverse transcription reaction was run for each extract and a no template reaction was included during each experiment. Melt curves yielded a single melt-peak for all template reactions and a minimal melt peak for the no template control reaction. Raw mRNA expression values were determined as being 2^{-CT}, where C_T is the second derivative of the fluorescence curve.

Immunocytochemistry

Expression of protein in pancreatic cancer cell lines was determined using the same primary antibodies used in the immunohistochemistry. Immunocytochemistry was done as reported previously by Lynch et al. (24). Secondary antibodies used were AlexaFluor488 goat anti-rabbit and AlexaFluor488 goat anti-mouse (Invitrogen). Following optimization, primary antibodies were diluted 1:50 and secondary antibodies were diluted 1:200. Cells were grown to 80% confluence on glass coverslips. Experiments were done in parallel; cells stained for each target were seeded, cultured, and stained simultaneously. Immunocytochemistry was done in duplicate for each cell line and primary antibody combination. Vectashield H-1000 mounting medium for fluorescence (Vector Laboratories) was used. Background labeling was determined by staining with only secondary antibody. Relative staining intensity compared with the no primary antibody control was recorded as +++ = high, ++ = moderate, and + = low.

To show coexpression of three targets in a single cell, a triple-label experiment was done. A coverslip of Capan-1 cells stained for PTPRR using AlexaFluor488 goat anti-rabbit secondary antibody was subsequently stained for PCDHB10 using goat anti-mouse Texas red secondary antibody (Invitrogen). The dual-stained coverslip was then blocked overnight using unlabeled goat anti-rabbit IgG (Sigma) at a 1:5 dilution. After blocking, the coverslip was stained for IL1RAP using Cy5 goat anti-rabbit secondary antibody (Jackson ImmunoResearch Laboratories) and mounted. The triple-labeled Capan-1 cells were then inspected and imaged for each target using an epifluorescence microscope using fluorochrome-specific excitation and emission wavelengths. A blocking control was done using a coverslip stained with AlexaFluor488 goat anti-rabbit secondary antibody. After blocking overnight, the control coverslip was stained using Cy5 goat anti-rabbit secondary antibody, mounted, and imaged. No Cy5 fluorescence was observed for the blocking control (data not shown).

Results

Microarray Gene Expression Profiling

We have generated microarray data for 103 normal tissue samples representing 28 different organ sites and 28 PanAdo tissue samples. The feature intensity values for each sample were normalized by the array median intensity. Consistent with observations of others (25), the internal stability of the data set was determined by multidimensional scaling analysis (Fig. 1A). Although obtained from different sources representing diverse ethnic, age, and gender groups, normal tissue samples belonging to the same organ type clustered together. Interestingly, the PanAdo samples did not always cluster together, indicating that gene expression patterns in pancreatic tumors are heterogeneous.

To facilitate data analysis and minimize target validation work, we curated a list of genes that encode proteins with

cell-surface epitopes or were predicted to be present on the cell surface by sequence homology or similarity. This list is limited to genes present on the Agilent Human 1A array. Because the Agilent 1A chips contain nearly every annotated gene (>18,000 genes), this list should represent most cell-surface proteins suitable for ligand discovery. Although it is acknowledged that this list is not necessarily complete, it represents our best attempt to assemble a list of cell-surface genes and was used herein to identify cell-surface target combinations specific for pancreatic cancer.

Area-Based Cutoff Values for Coverage Analysis

The frequency histogram of mRNA abundance followed a pseudo-power law (Fig. 1B). Thus, an important component of our analysis was identifying where to demarcate "expressed" genes from "nonexpressed." Although the level of mRNA expression is not always linearly related to the level of protein translation and subsequent localization to the cell surface, it is helpful to estimate the minimum level of mRNA expression that can lead to a level of protein at the cell surface sufficient for binding of an imaging or therapeutic agent. To make a best estimate, we adjusted the normal and tumor threshold values (see vertical lines in Fig. 1B) to maximize the stringency of the coverage analyses but still provide target combinations. The threshold values for normal tissues were defined as the intensity value below which proteins were considered
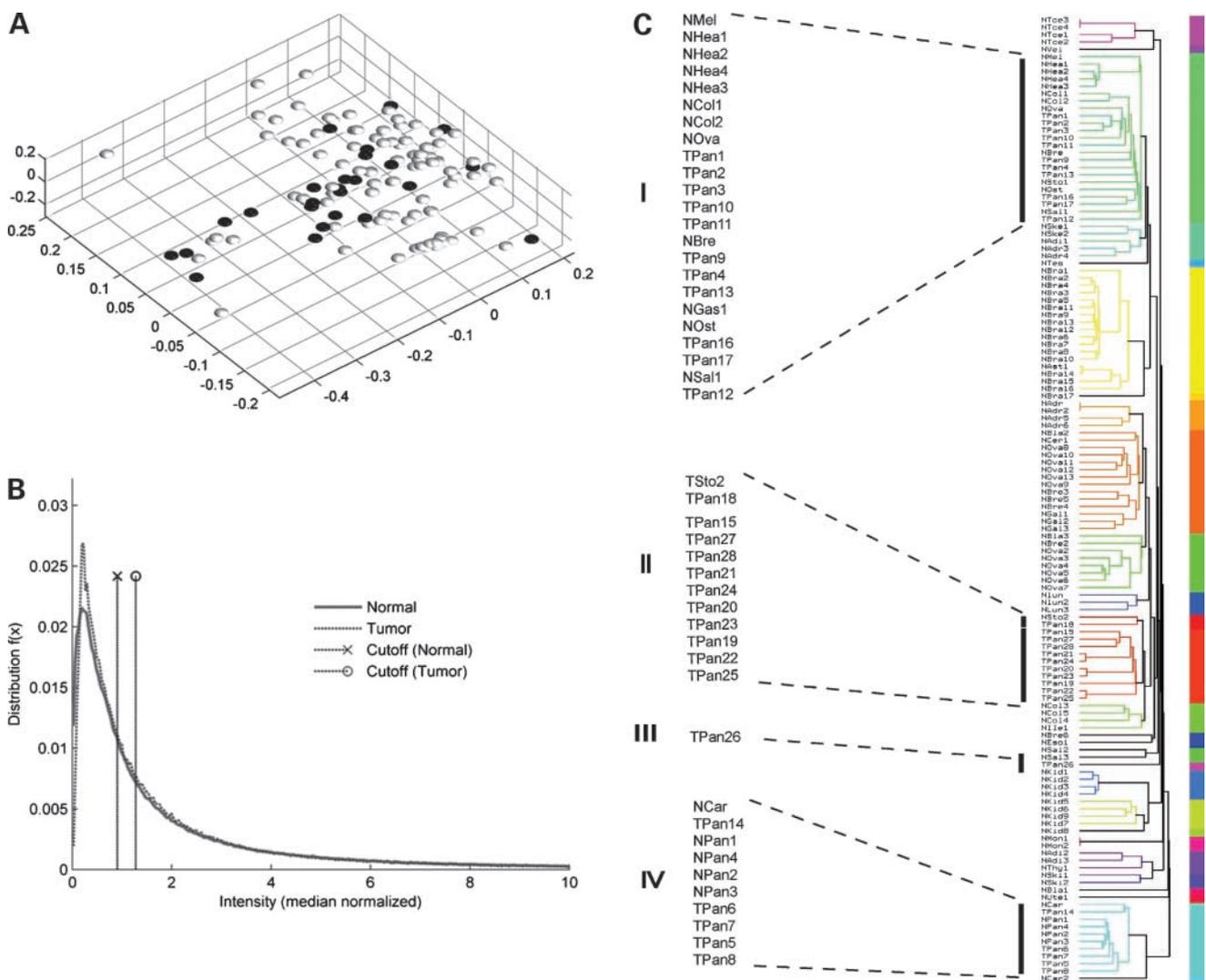
Figure 1. **A,** multidimensional scaling plots of the PanAdo tissues (*black dots*) and normal tissues (*gray dots*) based on microarray gene expression data. **B,** microarray intensity distribution plots of PanAdo samples (*dashed line*) and normal tissue samples (*solid line*). *Vertical lines,* cutoff values for demarcating a gene as either "expressed" in a given tumor sample (*dashed line with a circle*) or "not expressed" in a given normal sample (*dashed line with a cross*). **C,** dendrogram of PanAdo tissue groupings with normal tissues based on expression of cell-surface genes. *NMel,* normal melanocytes; *Nhea,* normal heart; *NCol,* normal colon; *NBre,* normal breast; *NOva,* normal ovary; *NOst,* normal osteoblasts; *NSal,* normal salivary gland; *NSke,* normal skeletal muscle; *NAdi,* normal adipose tissue; *NAdr,* normal adrenal gland; *NSto,* normal stomach; *NCar,* normal cartilage tissue; *NPan,* normal pancreas; *TPan,* PanAdo samples.

"not expressed." Similarly, the threshold values for tumor tissues were defined as the value above which proteins were considered "expressed." It was observed that, at normal threshold values above 0.55, extremely large numbers of combinations were identified. It was likewise observed that tumor threshold values greater than 0.75 led to the lack of identified combinations. Thus, area-based cutoffs that provided useful numbers of target combinations ranged from 0.35 to 0.55 for the normal tissues and 0.55 to 0.75 for tumor tissues. Combinations that provided the highest coverage among tumor tissues with the most stringent cutoff values were selected for further validation.

Algorithm Design for Target Identification

The avidity of a heteromultivalent ligand is determined by the affinities of the individual binding moieties combined with the presence and concentration of each target receptor on the cell surface. The specificity of a multimeric agent is largely determined by differences in the expression of each target protein between normal and tumor tissues. For example, a heterotrivalent ligand will bind more avidly to a cell that expresses all three complimentary cell-surface receptors compared with cells that express only two, or one, target proteins. Rose (26) and Barrett and Swindell (27) have determined that detection of an image detail by the human eye requires a signal intensity-to-noise ratio of at least 2. Thus, for imaging, a 3-fold signal enhancement in a target tissue relative to background enhancement is generally required for reliable detection. It is estimated that, for targeted therapies, a 100-fold increase in binding to target tissue relative to normal tissues is required (8, 28). Vagner et al. have reported that ligands exhibiting hetero-bivalent binding interactions show an ∼50-fold increase in binding relative to monovalent interactions (13).

From these observations, we estimated that a difference of 2 in the number of proteins targeted by heteromultimeric ligands in tumor tissue relative to normal tissues should provide a discriminating power that is sufficient for therapy or imaging. Thus, to identify gene combinations that will be useful for multimeric ligands, we invoked a "N - 2" rule; if a gene combination contains N genes and the tumor expresses all N genes, no more than N - 2 genes may be expressed in any given normal tissue [if it is a two-gene combination, the gene(s) must not be expressed in any normal tissues]. To identify target combinations that meet this rule, we first binarized the expression of the cell-surface genes to "not expressed" or "expressed" for each tissue sample using area-based cutoff values with the highest possible stringency (see above).

To identify the target combinations, a coverage flag was assigned to each tumor sample for each possible combination. If a tumor sample expresses all N targets in a given combination, it was assigned the flag "1"; otherwise, it was assigned "0." Likewise, if a normal tissue expresses more than N - 2 genes, it was assigned "1"; otherwise, it was assigned "0." Combinations with coverage flag "1" in any normal tissue were subsequently eliminated. The remaining combination was then ranked by the sum of coverage flags for all tumor samples. Thus, the highest ranked combinations were predicted to cover the most tumors and have little or low avidity to all normal tissues. As higher-dimensional combinations are computed, it is possible that the same tumor samples could be covered by lower-dimensional combinations. To only select combinations that covered more tumor samples than any lower-dimensional combinations, we introduced the Coverage Measurement (ψ) to quantify each combination. If ψ_q is the Coverage Measurement for qth dimension, then a combination with q + 1 dimensions is said to have an improvement in coverage over a combination with q dimensions only if $\psi_{q+1} > \psi_q$. Only combinations with a higher Coverage Measurement than all combinations with lower dimensions ($\psi_{q+1} > \max\{\psi_1, \psi_2, \ldots, \psi_q\}$) were selected as valid target combinations.

Target Combinations

Using this N - 2 rule-based algorithm, we have identified a list of 3-gene (Table 1) and 4-gene (Table 1) combinations that each cover at least 3 of 28 (11%) of the PanAdo samples. Many of these combinations share the same 1 or 2 genes. These common genes are not expressed in the majority of the normal tissues but require additional genes to differentiate the tumor samples from all normal tissues. Target combinations that contain 5 or more genes can be generated using the same computational methods. Interestingly, the algorithm did not identify any 2-gene combinations, indicating that there are no 2 genes that do not express in any of the normal tissues and that have a higher Coverage Measurement in tumor samples than either of the genes themselves at the cutoff levels we used. The number of possible combinations increases exponentially as the number of targets contained in a given combination increases.

Grouping of Pancreatic Cancer Based on Cell-Surface Expression

To characterize the heterogeneity of the pancreatic cancer tissues in terms of cell-surface expression, we did cluster analyses of all normal and tumor samples using microarray data corresponding to our list of cell-surface genes. Dendrograms were generated that show clustering of the PanAdo tissues into four groups by cell-surface expression (Fig. 1C). The majority (96%) of the tumor tissues were represented by three major groupings (I, II, and IV). Group II contains two very close clusters (the Nsto2/TPan18 cluster and the TPan16/TPan19-TPan25/TPan27-TPan28 cluster). Group IV tumors clustered with the normal pancreatic tissues, indicating that these tumors may be difficult to distinguish from normal pancreas by cell-surface expression or that the tumor biopsy samples in group IV contained a high percentage of normal tissue. Groups I and II each represent 39% of the tumor samples. As further evidence that these groupings are relevant, the 3- and 4-gene combinations that were identified as having the broadest coverage (Table 1) predominantly covered tumors in the tightly clustered group II. However, as evidence of some overlapping among the groups, three of the 3-gene combinations and one of 4-gene combinations

also covered the single tumor in group III and three of the 4-gene combinations covered one tumor in group I. Together, the identified combinations covered 100% of the group II tumors. Most tumors in group I were covered in 4-gene combinations that were ranked lower than the ones selected for further validation, and many of these combinations included two tumors from group I. Five tumors did not appear in any combinations identified by these analyses, one from group I and four of the five from group IV. Hence, these analyses provided combinations covering 82% of the PanAdo tissues tested.

Validation of Targets Using TMAs

To further validate the target combinations, we did TMA-based immunohistochemistry to examine protein levels of the targets in tissue samples. TMAs constructed from pancreatic cancer and normal tissues were used. The pancreatic cancer TMA contained 52 cases of pancreatic ductal adenocarcinomas, each of which was represented by at least two tumor cores. In addition, 38 of these cases were represented by a core from the matching adjacent normal region. The TMA also included 4 cases of normal pancreas from individuals with healthy pancreas. The normal tissue TMA contained 282 cores representing 66 different normal tissue types.

Commercial antibodies for targets of two 3-gene combinations were obtained for immunostaining: PTPRR, PCDHB10, IL1RAP, and SLC2A13. Immunostaining was done using optimized conditions and was scored by a board-certified pathologist (G.H.). Results for the PanAdo TMA are summarized in Table 2. All four targets showed strong staining in most tumor tissues and minimal or no staining in adjacent normal tissues. PTPRR was highly

($\geq$2+) expressed in 75% of the tumor cases, whereas only 10% of the adjacent normal tissues showed the similar level of staining. Thirty-seven percent of the tumor cases had $\geq$2+ staining for PCDHB10 and only 1 of 35 (3%) evaluable adjacent normal tissues showed 2+ staining. About 50% of the tumor cases showed $\geq$2+ expression for IL1RAP and a similar number of cases showed $\geq$2+ SLC2A13 staining. In contrast, almost all adjacent normal cases (except one case for SLC2A13, which was stained 2+) expressed these two targets at low levels (0 or 1+). None of the targets were stained more than 1+ in the normal pancreas tissues (Table 2). Overall, among the 46 tumor cases that were evaluable for all three members of the PTPRR, PCDHB10, and IL1RAP combination, 15 of them (33%) were stained $\geq$2+ for all three targets and 38 of them (82%) expressed all three at $\geq$1+ level. Likewise, among the 46 tumor cases that were evaluable for all three targets in the PTPRR, PCDH10, and SLC2A13 combination, 8 (17%) expressed all three targets at $\geq$2+ level and 35 (76%) expressed all three at $\geq$1+ level. The percentage of positive ($\geq$1+) staining for the combinations are much higher than the percentage of tumor coverage calculated from the microarray data, but the percentages of $\geq$2+ cases in the immunohistochemistry are only 2- or 3-fold higher than those from the microarray coverage analyses (11% for both combinations). This lower estimate of coverage by the microarray analysis is expected because we used cutoff values with the highest possible stringency in parsing the microarray data (see above). Representative staining of the targets in ductal PanAdo tissues and normal ductal pancreatic tissues are shown in Fig. 2A and B, respectively. PTPRR staining was mostly cytoplasmic. Borderline ductal tumor lesions and dilating

Table 1. Top 3-gene and 4-gene combinations identified based on microarray data analyses

Combination		Gene symbols				Tumor coverage by cluster analysis grouping (see Fig. 1C)
3-gene combinations	1	TM4SF4	PCDHB10	FCGR1A		Group II: TPan21, TPan22, TPan24, and TPan25
	2	IL1RAP	PCDHB10	SLCO1B3		Group II: TPan21, TPan22, TPan24, and TPan25
	3	PTPRR	IL1RAP	PCDHB10		Group II: TPan22 and TPan25
						Group III: TPan26
	4	IL1RAP	PCDHB10	SLC2A13		Group II: TPan22 and TPan25
						Group III: TPan26
	5	TM4SF4	PCDHB10	SLC2A13		Group II: TPan22 and TPan25
						Group III: TPan26
	6	PCDHB10	FCGR1A	SLCO1B3		Group II: TPan21, TPan22, TPan24, and TPan25
	7	CLEC4A	PCDHB10	SLCO1B3		Group II: TPan21, TPan22, TPan24, and TPan25
4-gene combinations	1	TM4SF4	FCGR1A	ASGR1	IL1RAP	Group II: TPan19, TPan21, TPan22, TPan24, TPan25, and TPan27
	2	TM4SF4	PCDHB10	PCDHB9	IL1RAP	Group II: TPan21, TPan22, TPan24, and TPan25
						Group III: TPan26
	3	TNFSF4	TM4SF4	MGC34923	TGFBR1	Group II: TPan15, TPan19, TPan22, TPan25, and TPan27
	4	PCDHB8	HLA-DQA1	PCDHB10	SLCO1B3	Group II: TPan18, TPan21, TPan22, TPan24, and TPan25
	5	PTPRR	PTPRC	SLCO1B3	ASGR1	Group I: TPan10
						Group II: TPan20, TPan22, TPan23, TPan25, and TPan28
	6	PTPRR	MS4A4A	SLCO1B3	ASGR1	Group I: TPan10
						Group II: TPan20, TPan22, TPan23, TPan25, and TPan28
	7	PTPRR	CEACAM6	MS4A4A	SLCO1B3	Group I: TPan10
						Group II: TPan20, TPan22, TPan23, TPan25, and TPan28

**Table 2.** Summary of pancreatic tumor TMA immunostaining results for four targets

Target	Sample classification	Score					% Cases with ≥2+
		0	1+	2+	3+	NE	
PTPRR	Normal	2	2	0	0	0	0
	Adjacent normal	7	21	3	0	7	10
	Tumor	0	12	28	8	4	75
PCDHB10	Normal	3	1	0	0	0	0
	Adjacent normal	7	27	1	0	3	3
	Tumor	1	21	22	4	4	37
IL1RAP	Normal	4	0	0	0	0	0
	Adjacent normal	24	5	0	0	9	0
	Tumor	6	19	18	5	4	48
SLC2A13	Normal	2	0	0	0	2	0
	Adjacent normal	20	10	1	0	7	3
	Tumor	7	18	18	4	5	47

Abbreviation: NE, net evaluable.

ducts had moderate staining (scored 1-2+). Staining for IL1RAP was also mostly cytoplasmic. Borderline tumors had quite strong staining (2-3+). Some acinar cells also stained positive for IL1RAP. Staining for PCDHB10 was also mostly cytoplasmic. Borderline tumor cells generally had strong staining (scored 2-3+). Pancreas acinar cells were also modestly positive for PCDHB10. Staining for

SLC2A13 was both membranous and cytoplasmic. Borderline tumors were modestly positive for SLC2A13.

Staining results for the four targets in the normal TMA was more complex than for the tumor TMA, as the normal TMA represented a variety of tissue types. All four targets had positive staining in certain normal tissue types, but the staining intensity was relatively weak (mostly 1+ or 2+).
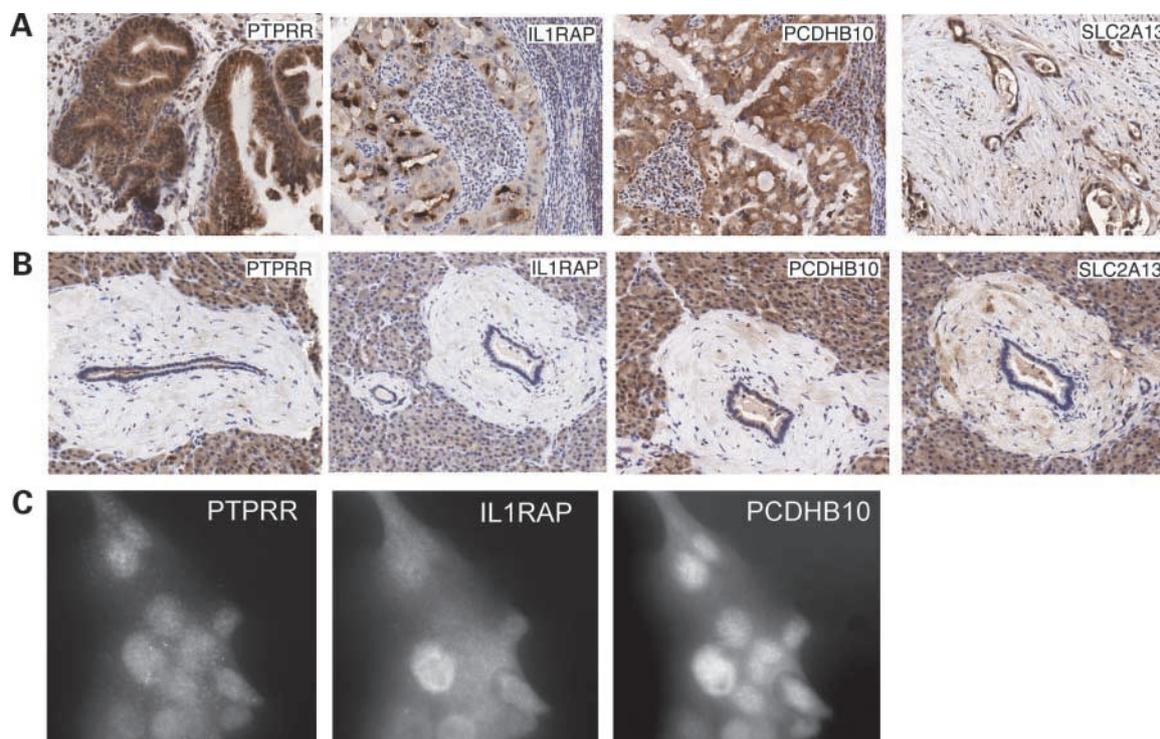
Figure 2. Validation of target combinations by immunohistochemistry in TMAs and immunohistochemistry in the Capan-1 pancreatic cancer cell line. **A,** representative immunohistochemical staining images of four targets, PTPRR, IL1RAP, PCDHB10, and SLC2A13, in ductal pancreatic tumor tissues. **B,** representative immunohistochemical staining images of the four targets in normal pancreatic ducts. **C,** triple-label immunohistochemistry showing coexpression of all three targets of the PTPRR, IL1RAP, and PCDHB10 combination in the same set of Capan-1 pancreatic cancer cells.

Table 3. Summary of immunostaining results on normal TMA for two target combinations

Tissue type	Combination 1			Combination 2		
	PTPRR	IL1RAP	PCDHB10	IL1RAP	PCDHB10	SLC2A13
Gastric mucosa	3+	1+	1+	1+	1+	1+
Small intestine*	0	2+	1+	2+	1+	0
Epididymis*	1+	1+	1+	1+	1+	0
Seminiferous tubules*	1+	0	2+	0	2+	0
Gallbladder	1+	1+	0	1+	0	0
Salivary gland	1+	0	1+	0	1+	0
Hair follicles*	0	1+	1+	1+	1+	0
Fallopian tube*	2+	2+	1+	2+	1+	0
Adrenal gland	1+	0	3+	0	3+	1+
Bronchial cartilage*	1+	0	1+	0	1+	0
Uterus smooth muscle	1+	0	1+	0	1+	0
Ovary, corpus luteum	1+	1+	1+	1+	1+	0
Placenta*	1+	1+	1+	1+	1+	0
Appendix*	0	1+	1+	1+	1+	1+
Bronchial epithelium	1+	0	1+	0	1+	0
Kidney	1+	0	2+	0	2+	1+
Bladder epithelium	1+	2+	1+	2+	1+	1+

*Tissue types that were not included in microarray expression profiling.

The gastric mucosa and vessel structures of placenta, uterus, and heart myocardium were stained positive for PTPRR. Weak staining of PTPRR was also seen in the adrenal gland, salivary gland, and genital tract structures such as seminal vesicles and fallopian tubes. Gastric mucosa and small intestine were focally positive for IL1RAP. Pancreas acinar cells were modestly stained for IL1RAP. Positive staining for IL1RAP was also observed in genital tracts such as epididymis, fallopian tubes, and corpus luteum of ovary. Most gastrointestinal tract tissues were stained positive for PCDHB10. The adrenal and kidney were also stained strong for PCDHB10 (2-3+). Staining of SLC2A13 was not as extensive as the other three targets. Only weak staining was seen in lymphatic endothelium, bladder endothelium, kidney medulla, adrenal gland, and gastric mucosa (Table 3).

There are a few tissue types that stained positive for two or three of the targets in each combination. As shown in Table 3, 17 tissue types had positive staining for two of the three targets in the PTPRR, IL1RAP, and PCDHB10 combination. Likewise, there are 11 tissue types that were positive for at least two of the three targets in the PTPRR, IL1RAP, and SLC2A13 combination. As described earlier, these two target combinations were identified based on the DNA microarray profiling data on 28 different normal tissue types. The microarray data analysis predicted that not more than one target would be expressed in any of the 28 normal tissue types. Although most of the tissue types that showed positive immunohistochemistry staining for two or more targets were not included in our DNA microarray profiling study, there are some tissue types that appear to be inconsistent between RNA expression (DNA microarray) and protein expression (immunohistochemistry).

Coexpression of Targets in Pancreatic Cancer Cell Lines

Because targets were validated in tumor tissue samples that have a heterogeneous mixture of cell types, determination of target expression in existing pancreatic cancer cell lines would serve as further validation. Microarray data were generated for 11 PanAdo cell lines. From these data, 5 lines (AsPC-1, Capan-1, HPAFII, PSN-1, and SU86.86) were selected that may express all three targets in at least one of the validated three-gene combinations. Expression of the four validated targets (IL1RAP, PCDHB10, PTPRR, and SLC2A13) was determined quantitatively at the level of mRNA by quantitative real-time reverse transcription-PCR and qualitatively at the level of protein by immunohistochemistry (Table 4). Cell lines were identified that expressed all three targets in both validated combinations (e.g., AsPC-1 and Capan-1 cells express targets for both combinations at relatively high levels). For the IL1RAP-PCDHB10-PTPRR combination, Capan-1 cells expressed mRNA ranging from 0.006 to 0.05 level of ACTB (β-actin) mRNA and showed relatively high staining for all three targets by immunohistochemistry. Because cultures used for immunohistochemistry were seeded and stained simultaneously, and 100% of cells were stained for each target, it is unlikely that staining for each target was due to staining of discrete subpopulations within each culture. Hence, it can be concluded from these data that the targets are coexpressed in these cells.

To verify coexpression in the same cells, triple-label immunohistochemistry was done for all three targets in the IL1RAP-PCDHB10-PTPRR combination on Capan-1 cells using secondary antibodies with spectrally distinct fluorochromes. As shown in Fig. 2C, Capan-1 cells showed coexpression of these three targets, and staining is observed throughout the cell for all three targets.

Discussion

We report the identification of gene combinations that can be used to develop multitargeted ligands using DNA microarray-based gene expression profiling. Each combination contains genes that are concurrently expressed in pancreatic cancer but not in a variety of normal tissue types including normal pancreas. Genes included in the combination list are either known to encode cell-surface proteins or are predicted to encode proteins with transmembrane (plasma membrane) domains based on database annotations. We sought to overcome one of the potential pitfalls of DNA microarray-based target identification wherein mRNA levels do not always correlate with protein levels at the cell surface by examining the protein levels of two of the 3-gene combinations by TMA-based immunohistochemistry. Protein expression levels of the targets were consistent with the DNA microarray data in PanAdo tissues and in a majority of normal tissues. However, there was a subset of normal tissues that showed expression of two or more targets in the 3-gene combinations. There are possible explanations for such discrepancies: (*a*) it could be that target mRNA expression levels are not correlated with protein expression in some tissue types; (*b*) some tissue types, such as the adrenal gland, are highly immunoreactive and the immunohistochemistry signal might not be target specific; and (*c*) differences might be due to the fact that the microarray study tissues were not dissected for different cell types, whereas in the immunohistochemical evaluation the intensity score was based on the cell types that exhibited the strongest staining. Further study is needed to pinpoint the exact reason.

Multimeric ligand targeting of cancer is based on the premise that cell-surface target combinations highly specific to tumor cells can be identified. Several studies have reported gene expression profiles of pancreatic cancers using various approaches. Typically, many cell-surface genes/proteins were identified as up-regulated in pancreatic cancer relative to normal pancreas. However, very few of these genes were validated as imaging targets mainly due to their low specificity against normal tissues besides pancreas. Our approach for identifying cell-surface targets is different from other approaches in that we emphasize low or no target expression among all normal tissue types rather than high expression in tumor tissues. Due to the unique binding kinetics of multimeric ligands, a high level of expression for individual targets is desired but may not be absolutely required. Although the binding of multimeric ligands to their targets could be complicated, it is expected that multimeric ligands will have increased binding compared with monomeric ligands. This increase in avidity can be attributed to a variety of different factors including an increased local, or effective, concentration of ligand following binding of the first ligand of the multimer and decreased off-rates of a multimeric ligand, resulting in an apparent cooperativity (8, 10, 13). This suggests that the affinity of each individual ligand for binding the respective target need not be very high.

For a multimeric ligand to be effective, it requires the targets be concurrently expressed on the cell surface of tumor cells. As a result, a target combination might cover a lower percentage of patients compared with single targets. We found that the highest percentage of patient tumors covered by a target combination is 11% for 3-gene combinations and 21% for 4-gene combinations. Hence, multiple combinations are needed to treat all patients with a general classification of disease. This study identified combinations that together covered 82% of the PanAdo tissues analyzed. Of the 18% of tumors not covered, 80% of them clustered in group IV (Fig. 1C) with normal pancreas tissue. The number of combinations needed to cover a majority of pancreatic cancers is difficult to predict, because there is some overlap in coverage among target combinations. Because most of the targets identified in this study do not already have ligands suitable for the assembly of multimeric ligands, further progress will require the development of ligands for each individual target, which is not a trivial task. Determining the exact number of combinations that will be required is somewhat dependent on real progress in the development of specific ligands.

In summary, our results show that target combinations that are potentially very selective for a certain cell type (PanAdo cells in this case) can be identified using an approach combining DNA microarray expression profiling and TMA-based immunohistochemistry. We are currently in the process of developing multimeric ligands for target combinations identified herein to further validate our targeting strategy.

Table 4. Coexpression of validated targets in pancreatic cancer cell lines

Target	IL1RAP		PCDHB10		PTPRR		SLC2A13	
Cell line	mRNA (SE)*	Protein[†]	mRNA (SE)*	Protein[†]	mRNA (SE)*	Protein[†]	mRNA (SE)*	Protein[†]
AsPC-1	1.9 (0.1)	+++	13 (3)	+++	57 (10)	+++	90 (10)	+++
Capan-1	12 (2)	+++	5.5 (0.8)	+++	46 (8)	+++	1.5 (0.8)	+++
HPAFII	0.63 (0.1)	+++	2.0 (0.3)	++	26 (5)	+++	5.9 (4)	+++
PSN-1	0.70 (0.1)	+++	0.044 (0.004)	++	0.1 (0.09)	++	11 (0.6)	++
SU86.86	0.62 (0.1)	+	0.009 (0.005)	++	2.3 (0.1)	++	0.39 (0.1)	++

*Normalized to ACTB (β-actin) expression [(target gene 2^{-CT}/ACTB 2^{-CT}) × 1,000]. Mean (SE) of three samples.
[†] Relative staining intensity compared with no primary antibody control: +++ = high, ++ = moderate, and + = low. Controls had no staining.

Disclosure of Potential Conflicts of Interest

No potential conflicts of interest were disclosed.

References

1. Temming K, Schiffelers RM, Molema G, Kok RJ. RGD-based strategies for selective delivery of therapeutics and imaging agents to the tumour vasculature. Drug Resist Updat 2005;8:381 – 402.

2. Haubner R, Weber WA, Beer AJ, et al. Noninvasive visualization of the activated $\alpha_v\beta_3$ integrin in cancer patients by positron emission tomography and [^{18}F]galacto-RGD. PLoS Med 2005;2:e70.

3. Beer AJ, Haubner R, Wolf I, et al. PET-based human dosimetry of ^{18}F-galacto-RGD, a new radiotracer for imaging $\alpha_v\beta_3$ expression. J Nucl Med 2006;47:763 – 9.

4. Goldenberg DM, Sharkey RM. Novel radiolabeled antibody conjugates. Oncogene 2007;26:3734 – 44.

5. Jhanwar YS, Divgi C. Current status of therapy of solid tumors. J Nucl Med 2005;46 Suppl 1:141 – 50S.

6. Goldenberg DM, Sharkey RM. Advances in cancer therapy with radiolabeled monoclonal antibodies. Q J Nucl Med Mol Imaging 2006; 50:248 – 64.

7. Boturyn D, Coll JL, Garanger E, Favrot MC, Dumy P. Template assembled cyclopeptides as multimeric system for integrin targeting and endocytosis. J Am Chem Soc 2004;126:5730 – 9.

8. Handl HL, Vagner J, Han H, Mash E, Hruby VJ, Gillies RJ. Hitting multiple targets with multimeric ligands. Expert Opin Ther Targets 2004;8: 565 – 86.

9. Laugel B, Boulter JM, Lissin N, et al. Design of soluble recombinant T cell receptors for antigen targeting and T cell inhibition. J Biol Chem 2005;280:1882 – 92.

10. Vagner J, Handl HL, Gillies RJ, Hruby VJ. Novel targeting strategy based on multimeric ligands for drug delivery and molecular imaging: homooligomers of α-MSH. Bioorg Med Chem Lett 2004;14:211 – 5.

11. Garanger E, Boturyn D, Coll JL, Favrot MC, Dumy P. Multivalent RGD synthetic peptides as potent $\alpha_v\beta_3$ integrin ligands. Org Biomol Chem 2006;4:1958 – 65.

12. Caplan MR, Rosca EV. Targeting drugs to combinations of receptors: a modeling analysis of potential specificity. Ann Biomed Eng 2005;33: 1113 – 24.

13. Vagner J, Xu L, Handl HL, et al. Heterobivalent ligands crosslink multiple cell-surface receptors: the human melanocortin-4 and δ-opioid receptors. Angew Chem Int Ed Engl 2008;47:1685 – 8.

14. Boyd RS, Adam PJ, Patel S, et al. Proteomic analysis of the cell-surface membrane in chronic lymphocytic leukemia: identification of two novel proteins, BCNP1 and MIG2B. Leukemia 2003;17:1605 – 12.

15. Zhao Y, Zhang W, Kho Y. Proteomic analysis of integral plasma membrane proteins. Anal Chem 2004;76:1817 – 23.

16. Loyet KM, Ouyang W, Eaton DL, Stults JT. Proteomic profiling of surface proteins on Th1 and Th2 cells. J Proteome Res 2005;4:400 – 9.

17. Tangrea MA, Wallis BS, Gillespie JW, Gannot G, Emmert-Buck MR, Chuaqui RF. Novel proteomic approaches for tissue analysis. Expert Rev Proteomics 2004;1:185 – 92.

18. Dougherty ER, Barrera J, Brun M, et al. Inference from clustering with application to gene-expression microarrays. J Comput Biol 2002;9: 105 – 26.

19. Kononen J, Bubendorf L, Kallioniemi A, et al. Tissue microarrays for high-throughput molecular profiling of tumor specimens. Nat Med 1998; 4:844 – 7.

20. Andersen CL, Hostetter G, Grigoryan A, Sauter G, Kallioniemi A. Improved procedure for fluorescence *in situ* hybridization on tissue microarrays. Cytometry 2001;45:83 – 6.

21. Mousses S, Bubendorf L, Wagner U, et al. Clinical validation of candidate genes associated with prostate cancer progression in the CWR22 model system using tissue microarrays. Cancer Res 2002;62:1256 – 60.

22. Watanabe A, Cornelison R, Hostetter G. Tissue microarrays: applications in genomic research. Expert Rev Mol Diagn 2005;5:171 – 81.

23. Morse DL, Carroll D, Weberg L, Borgstrom MC, Ranger-Moore J, Gillies RJ. Determining suitable internal standards for mRNA quantification of increasing cancer progression in human breast cells by real-time reverse transcriptase polymerase chain reaction. Anal Biochem 2005; 342:69 – 77.

24. Lynch RM, Fogarty KE, Fay FS. Modulation of hexokinase association with mitochondria analyzed with quantitative three-dimensional confocal microscopy. J Cell Biol 1991;112:385 – 95.

25. Son CG, Bilke S, Davis S, et al. Database of mRNA gene expression profiles of multiple human organs. Genome Res 2005;15:443 – 50.

26. Rose A. The sensitivity performance of the human eye on an absolute scale. J Opt Soc Am 1948;38:196.

27. Barrett HH, Swindell W. Noise in images. In: Barrett HH, Swindell W, editors. Radiological imaging. Academic Press; 1981. p. 494 – 560.

28. Mammen M, Choi S-K, Whitesides GM. Polyvalent interactions in biological systems: implications for design and use of multivalent ligands and inhibitors. Angewandte Chemie 1998;37:2754 – 96.

Molecular Cancer Therapeutics

Gene expression profiling-based identification of cell-surface targets for developing multimeric ligands in pancreatic cancer

Updated version	Access the most recent version of this article at: doi:10.1158/1535-7163.MCT-08-0402
Supplementary Material	Access the most recent supplemental material at: http://mct.aacrjournals.org/content/suppl/2008/09/05/1535-7163.MCT-08-0402.DC1

E-mail alerts	Sign up to receive free email-alerts related to this article or journal.
Reprints and Subscriptions	To order reprints of this article or to subscribe to the journal, contact the AACR Publications Department at pubs@aacr.org.
Permissions	To request permission to re-use all or part of this article, use this link http://mct.aacrjournals.org/content/early/2005/11/01/1535-7163.MCT-08-0402.citation. Click on "Request Permissions" which will take you to the Copyright Clearance Center's (CCC) Rightslink site.